DALTON
FULL PAPER

Magnetic properties and crystal structures of bis(μ-pyrazolato)-bridged dicopper(II,II) complexes with 1,10-phenanthroline or 2,2′-bipyridine

Hideaki Matsushima, Hironobu Hamada, Kanna Watanabe, Masayuki Koikawa and Tadashi Tokii *

Department of Chemistry and Applied Chemistry, Faculty of Science and Engineering, Saga University, Saga 840-8502, Japan

Received 19th October 1998, Accepted 19th January 1999

Novel bis(μ-pyrazolato)-bridged binuclear copper(II) complexes with 1,10-phenanthroline (phen) or 2,2′-bipyridine (bpy), $Cu_2(NO_3)_2(L)_2(L')_2{\cdot}n(H_2O$ or MeOH), where L = pyrazolate (pz), 4-methylpyrazolate (4-Mepz), 4-chloropyrazolate (4-Clpz), or 4-bromopyrazolate (4-Brpz) anions and L′ = phen or bpy, were prepared and characterized by electronic spectra, magnetic susceptibilities and X-ray structure analyses. The crystal structures of $[Cu_2(NO_3)(pz)_2(H_2O)(phen)_2]NO_3$ **1**, $[Cu_2(NO_3)_2(pz)_2(phen)_2]$ **2**, $[Cu_2(NO_3)_2(4\text{-Clpz})_2(phen)_2]{\cdot}2MeOH$ **3**·2MeOH, $[Cu_2(NO_3)_2(4\text{-Brpz})_2(phen)_2]{\cdot}2MeOH$ **4**·2MeOH, $[Cu_2(4\text{-Mepz})_2(H_2O)_2(bpy)_2][NO_3]_2$ **5** and $[Cu_2(4\text{-Mepz})_2(H_2O)_2(phen)_2][NO_3]_2$ **6** were determined by X-ray crystallography. All of the complexes consist of a discrete binuclear molecule with bis(μ-pyrazolato)-bridges. Complexes **1**, **2**, **3**·2MeOH and **4**·2MeOH have a distorted trigonal-bipyramidal configuration around each copper(II) ion. On the other hand, complexes **5** and **6** have a distorted square-bipyramidal geometry, and reside on a mirror plane so that one half of the molecule is crystallographically unique. The bending angles ($\delta_{pz\text{-}bend}$) of the pyrazolato-bridges in **1**–**6**, which represent dihedral angles of the least-squares plane of pz relative to the Cu–N(pz)–N(pz)–Cu plane, are in the 1.4–9.7° range. The angular structural parameters (τ) for **1**–**6**, which are applicable to five-coordinate structures as an index of the degree of trigonality, are in the 0.10–0.76 range. The magnetic susceptibility data for **1**–**6** conform to the usual dimer equation with $-2J$ values of 143–268 cm^{-1}, indicating the existence of an antiferromagnetic interaction. The strength of the antiferromagnetic interaction for **1**–**6** is correlated with $\delta_{pz\text{-}bend}$ and τ values. The τ value is a leading factor in determining the $-2J$ value, and the bending angle ($\delta_{pz\text{-}bend}$) plays an important supporting part.

There is continuing interest in understanding the relationship between structural features and the strength of magnetic exchange interactions in symmetrical di-bridged copper(II) dimers. While a linear relationship exists in bis(μ-hydroxo)- or bis(μ-alkoxo)-bridged binuclear copper(II) complexes between the magnetic-exchange coupling constant, J, and the Cu–O–Cu bond angles,[1] the same degree of understanding has not been achieved for two-atom-bridged species yet. It is well known that a pyrazolate anion functions as a two-atom-bridging group through its two nitrogen atoms.[2] The pyrazolate bridge in binuclear copper(II) complexes generally appears in combination with another bridging group such as alkoxo, phenoxo, thiolato, thiophenolato, acetato, azido, chloro or bromo.[3] Many pyrazole-bridged polymeric copper(II) complexes have been reported,[4] whereas binuclear copper(II) complexes having only pyrazolate anions as bridging ligands are still limited.[5] Although there are some "first examples" of bis(μ-pyrazolato)dicopper(II) complexes, such complexes are obtained by using pyrazole-based ligands with one or two chelating arm(s) attached to the pyrazole ring functioned as an endogenous bridging group. Drew *et al.* obtained binuclear copper(II) complexes with a bis(μ-pyrazolato)-bridged core by applying binucleating macrocycles which encourage the incorporation of pyrazolate anions as exogenous bridging ligands.[6] Unfortunately, no discrete binuclear copper(II) complex with only pyrazolate bridges has been characterized structurally and magnetically up until now. Thus, we describe herein the syntheses, crystal structures and magnetic properties of some genuine pyrazolate bridged binuclear copper(II) complexes.

Experimental

Materials

4-Chloropyrazole (4-ClpzH) and 4-bromopyrazole (4-BrpzH) were prepared by using the same procedure as described in the literature.[4b] All other chemicals and solvents were of reagent grade and were used without further purification.

Syntheses

$[Cu_2(NO_3)(pz)_2(H_2O)(phen)_2]NO_3$ 1. An aqueous solution (20 cm^3) of $Cu(NO_3)_2{\cdot}3H_2O$ (1.20 g, 5 mmol) and phen·H_2O (0.98 g, 5 mmol) was stirred for a few minutes. The pale green precipitate was filtered off, and to the filtrate was added a solution of pyrazole (pzH) (0.34 g, 5 mmol) in H_2O (5 cm^3). The resulting blue solution was adjusted to pH 4.4 with 1 mol dm^{-3} aqueous NaOH. The reaction mixture was stirred for 10 min at room temperature, and the light green precipitate was filtered off (**1**·$4H_2O$; yield 0.52 g). The filtrate was allowed to stand overnight at room temperature, and the resulting deep blue crystals were collected by filtration, washed with water, and dried in air; yield 1.18 g (Found: C, 47.21; H, 3.19; N, 18.33; Cu, 16.74. $C_{30}H_{24}Cu_2N_{10}O_7$ requires C, 47.18; H, 3.17; N, 18.34; Cu, 16.64%).

$[Cu_2(NO_3)_2(pz)_2(phen)_2]$ 2. This complex was obtained as deep green crystals by recrystallization of **1**·$4H_2O$ from methanol; yield 85% (Found: C, 48.33; H, 2.94; N, 18.80; Cu, 16.99. $C_{30}H_{22}Cu_2N_{10}O_6$ requires C, 48.32; H, 2.97; N, 18.78; Cu, 17.04%).

$[Cu_2(NO_3)_2(4\text{-}Clpz)_2(phen)_2]$ 3. To a solution of 4-chloropyrazole (0.20 g, 2 mmol) in methanol–acetonitrile (6:1) (9 cm^3) was added to a solution of $Cu(NO_3)_2 \cdot 3H_2O$ (0.48 g, 2 mmol) in methanol–acetonitrile (6:1) (11 cm^3). The mixture was stirred at 40 °C for 20 min, and to this were added triethylamine (2 mmol) and a solution of phen·H_2O (0.40 g, 2 mmol) in methanol–acetonitrile (6:1) (7 cm^3). The green precipitate was filtered off. The filtrate was allowed to stand for one week to give deep green crystals, which were collected by filtration, washed with methanol, and dried *in vacuo*; yield 0.43 g (Found: C, 44.04; H, 2.49; N, 17.15; Cu, 15.67. $C_{32}H_{28}Cl_2Cu_2N_{10}O_8$ requires C, 44.24; H, 2.47; N, 17.20; Cu, 15.60%).

$[Cu_2(NO_3)_2(4\text{-}Brpz)_2(phen)_2]$ 4. To a solution of 4-bromopyrazole (0.30 g, 2 mmol) in methanol–acetonitrile (3:1) (19 cm^3) was added a solution of $Cu(NO_3)_2 \cdot 3H_2O$ (0.48 g, 2 mmol) in methanol–acetonitrile (3:1) (20 cm^3). The mixture was stirred at 40 °C for 20 min, and to this were added triethylamine (2 mmol) and a solution of phen·H_2O (0.40 g, 2 mmol) in methanol–acetonitrile (3:1) (15 cm^3). The precipitate was filtered off. The filtrate was allowed to stand for one week to give deep green crystals, which were collected by filtration, washed with methanol, and dried *in vacuo*; yield 0.38 g (Found: C, 39.86; H, 2.25; N, 15.46; Cu, 14.15. $C_{32}H_{28}Br_2Cu_2N_{10}O_8$ requires C, 39.88; H, 2.23; N, 15.50; Cu, 14.07%).

$[Cu_2(4\text{-}Mepz)_2(H_2O)_2(bpy)_2][NO_3]_2$ 5. To a solution of bpy (0.31 g, 2 mmol) in methanol–water (1:1) (8 cm^3) $Cu(NO_3)_2 \cdot 3H_2O$ (0.48 g, 2 mmol) and 4-methylpyrazole (4-MepzH) (0.16 g, 2 mmol) were added. The reaction mixture was stirred for 20 min, and the resulting blue solution was adjusted to pH 4.6 with triethylamine. The deep green precipitate was collected by filtration, washed with water and methanol, and dried in air; yield 0.39 g. The product was recrystallized from methanol–ethanol (4:1) (Found: C, 44.10; H, 3.99; N, 18.29; Cu, 16.78. $C_{28}H_{30}Cu_2N_{10}O_8$ requires C, 44.15; H, 3.97; N, 18.39; Cu, 16.69%).

$[Cu_2(4\text{-}Mepz)_2(H_2O)_2(phen)_2][NO_3]_2$ 6. Copper(II) nitrate trihydrate (0.72 g, 3 mmol) and 4-methylpyrazole (0.49 g, 6 mmol) were slowly dissolved with stirring in a solution of phen·H_2O (1.19 g, 6 mmol) in methanol–water (1:1) (12 cm^3). After 20 min, the blue solution obtained was adjusted to pH 6.4 with triethylamine. The precipitate was filtered off. The filtrate was allowed to stand for one week to give deep green crystals, which were collected by filtration, washed with water and methanol, and dried in air; yield 0.24 g (Found: C, 47.44; H, 3.75; N, 17.32; Cu, 15.49. $C_{32}H_{30}Cu_2N_{10}O_8$ requires C, 47.47; H, 3.73; N, 17.30; Cu, 15.70%).

Physical measurements

The electronic spectra were recorded by the diffuse reflectance technique with a Hitachi 323 or Perkin-Elmer Lambda 19 recording spectrometer. The magnetic susceptibilities were determined by the Faraday method in the temperature range 80–300 K. The effective magnetic moments per copper ion at room temperature were calculated with eqn. (1), where χ_A is

$$\mu_{eff} = 2.83 \times \sqrt{(\chi_A - N\alpha)T} \quad (1)$$

the molar magnetic susceptibility corrected for diamagnetism of the constituent atoms using Pascal's constant,[7] and $N\alpha$ is the temperature-independent paramagnetism per mole of copper(II).

X-Ray crystal structure determination

The diffraction data were measured on a Rigaku AFC5S automated four-circle diffractometer with graphite-monochromated Cu-Kα ($\lambda = 1.54178$ Å) or Mo-Kα ($\lambda = 0.71069$ Å) radiation. The unit-cell parameters of each crystal were obtained from a least-squares refinement based on 25 high-angle reflections. The data were collected at a temperature of 23 ± 1 °C using the ω–2θ scan technique to a maximum 2θ value of 120° for Cu-Kα radiation and of 55° for Mo-Kα radiation. The crystal data and experimental conditions are shown in Table 1. The intensities of three representative reflections, which were measured after every 150 reflections, remained constant throughout data collection for **1**, **2**, **5** and **6**, indicating crystal and electronic stability (no decay correction was applied). Although each crystal of **3**·2MeOH and **4**·2MeOH was coated by epoxy resin to prevent efflorescence, the intensities of three representative reflections declined (16–18%). A linear correction factor was applied to the data to account for these phenomena. An empirical absorption correction based on azimuthal scans of several reflections was applied. The data were corrected for Lorentz and polarization effects.

The structures were solved by direct methods.[8] The non-hydrogen atoms were refined anisotropically, except for all carbon atoms of **4**·2MeOH and **6**. Refinements were carried out by the full-matrix least-squares method.[9] All hydrogen atoms were placed at geometrically idealized positions and were fixed in the refinements. The neutral atom scattering factors were taken from Cromer and Waber.[10] Anomalous dispersion effects were included in F_c;[11] the values for $\Delta f'$ and $\Delta f''$ were those of Cromer.[12] All calculations were performed using the TEXSAN[13] crystallographic software package.

CCDC reference number 186/1322.

Results and discussion

Crystal structures

The structures of complexes **1**–**6** are shown in Fig. 1(*a*)–1(*f*), respectively. The selected bond distances and angles for **1**, **2**, **3**·2MeOH and **4**·2MeOH are listed in Table 2, and those for **5** and **6** are listed in Table 3, respectively.

The structures of **1**–**6** consist of binuclear units with five-coordinated copper ions linked by only two pyrazolate ions. This type of binuclear copper complex having pyrazolate bridges is very unique, because the pyrazolate bridge in binuclear copper(II) complexes generally appears in combination with another bridging group.[3] The geometry of each copper atom in **1**–**4**·2MeOH is best described as a distorted trigonal bipyramid (*TBPY*) with the approximately linear trigonal-axes of N(1)–Cu(1)–N(5) and N(4)–Cu(2)–N(8): 174.9(2), 171.1(2)° for **1**; 172.4(4), 171.9(3)° for **2**; 170.8(2), 170.8(2)° for **3**·2MeOH; 170.7(5), 170.0(5)° for **4**·2MeOH, respectively. Complexes **2**, **3**·2MeOH and **4**·2MeOH have the same copper coordination sites with the equatorial plane comprised of a phen nitrogen, a pyrazolate nitrogen and a nitrate oxygen atom, whereas in **1** the two copper coordination sites are different to each other; in the Cu(2) site the water oxygen atom [O(4)] takes one equatorial position instead of the nitrate oxygen. Of the two nitrogen atoms of each pyrazolate ligand in **1**–**4**·2MeOH one occupies an axial position of one copper ion and the other occupies an equatorial site of the other copper ion. In **5** and **6**, the geometry at each copper atom is best described as a distorted square-pyramid (*SPY*). The basal positions are occupied by four nitrogen atoms [N(1), N(2), N(3), N(4)] of phen or bpy and pyrazolate, and the apical position is occupied by an oxygen atom [O(1)] of a water molecule [the two largest angles of 164.31(14)°, 170.13(14)° for **5** and 168.3(4)°, 159.8(4)° for **6**]. The Cu–O bond distances of 2.223(3) Å for **5** and 2.186(9) Å for **6** are in the range found for an axially coordinated water molecule. Addison *et al.*[14] have proposed an angular structural parameter, $\tau = (\beta - \alpha)/60$ [α and β ($\beta \geq \alpha$) are defined as the two largest angles in a five-coordinate system], which is applicable to five-coordinate structures as an index of the degree of trigonality. The τ value is equal to zero for a perfectly tetragonal geometry, while it becomes unity for a perfectly *TBPY* geometry. Judging from this criterion, the coordination geometry for **1**, **2**, **3**·2MeOH and **4**·2MeOH (the

Table 1 Crystallographic data and collection details

	1	**2**	**3**·2MeOH	**4**·2MeOH	**5**	**6**
Formula	$C_{30}H_{24}Cu_2N_{10}O_7$	$C_{30}H_{22}Cu_2N_{10}O_6$	$C_{32}H_{28}Cl_2Cu_2N_{12}O_8$	$C_{32}H_{28}Br_2Cu_2N_{10}O_8$	$C_{28}H_{30}Cu_2N_{10}O_8$	$C_{32}H_{30}Cu_2N_{10}O_8$
M	763.67	745.66	878.63	967.54	761.70	809.74
Crystal dimensions/mm	0.30 × 0.30 × 0.50	0.40 × 0.30 × 0.70	0.50 × 0.30 × 0.70	0.40 × 0.30 × 0.60	0.60 × 0.50 × 0.70	0.30 × 0.15 × 0.35
Crystal system	Triclinic	Monoclinic	Monoclinic	Monoclinic	Orthorhombic	Orthorhombic
Space group	$P\bar{1}$	$P2_1/n$	$P2_1/c$	$P2_1/c$	*Pnma*	*Pnma*
a/Å	9.865(8)	10.256(7)	17.155(24)	17.332(10)	15.162(6)	16.030(17)
b/Å	10.722(5)	14.924(13)	10.093(2)	10.104(9)	21.2111(12)	20.965(3)
c/Å	15.481(8)	19.291(5)	20.856(4)	20.853(6)	10.2870(9)	10.544(3)
α/°	78.21(4)					
β/°	103.28(6)	96.28(3)	98.63(6)	97.80(3)		
γ/°	106.38(5)					
V/Å^3	1511.9(17)	2935(2)	3570(5)	3618(4)	3308.3(14)	3544(4)
Z	2	4	4	4	4	4
D_c/g cm^{-3}	1.677	1.687	1.635	1.776	1.529	1.518
F(000)	776	1512	1784	1928	1560	1656
μ/cm^{-1}	22.66[a]	22.94[a]	14.08[b]	34.29[b]	13.49[b]	12.64[b]
Absorption correction:[c] T_{min}, T_{max}	0.416, 0.507	0.477, 0.502	0.577, 0.655	0.211, 0.357	0.418, 0.509	0.728, 0.827
No. of measured reflections	4739	4835	8952	5857	4278	3573
No. of observations	3575[d]	3240[d]	3771[d]	2447[e]	2150[d]	1300[f]
No. of variables	442	433	487	327	219	159
Final residuals:[g] R, R_w	0.067, 0.086	0.077, 0.110	0.057, 0.062	0.080, 0.066	0.041, 0.045	0.080, 0.078
Largest peak in final difference Fourier/e Å^{-3}	1.42	1.17	0.49	0.74	0.46	0.90

[a] Cu-Kα radiation. [b] Mo-Kα radiation. [c] ψ scan. [d] $I > 3\sigma(I)$. [e] $I > 1.5\sigma(I)$. [f] $I > 2\sigma(I)$. [g] $R = \sum||F_o| - |F_c||/\sum|F_o|$ and $R_w = [\sum w(|F_o| - |F_c|)^2/\sum wF_o^2]^{\frac{1}{2}}$.

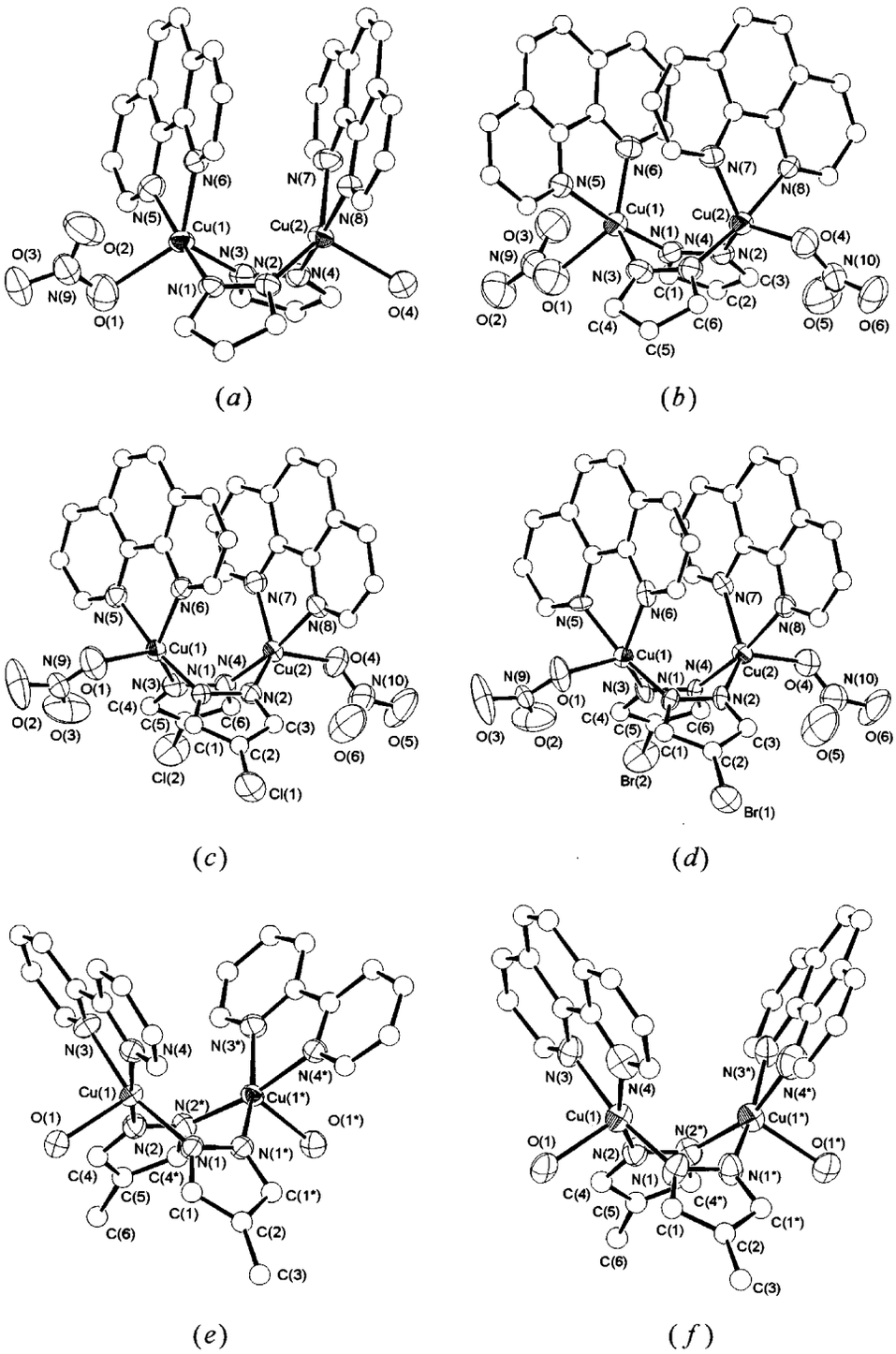

Fig. 1 The crystal structures of the complex cations of **1** (*a*), **5** (*e*), **6** (*f*) and complexes **2** (*b*), **3** (*c*), **4** (*d*). Thermal ellipsoids are at 50% probability level except for carbon atoms, which are represented as spheres of arbitrary size. Hydrogen atoms are not shown for clarity.

average τ values for two copper ion sites are 0.61, 0.63, 0.55 and 0.54, respectively) is described as a fairly distorted *TBPY* geometry, and the degree of distortion toward *SPY* in **3**·2MeOH and **4**·2MeOH is greater than that in **1** and **2**. The geometry for **5** ($\tau = 0.10$) and **6** ($\tau = 0.14$) is better described as *SPY*.

It can be seen from Table 2 that the three bond angles in each equatorial plane of **1**, **2**, **3**·2MeOH and **4**·2MeOH deviate appreciably from the 120° expected for the idealized *TBPY* geometry. In addition, each copper ion slightly deviates from the equatorial planes towards the pyrazolate nitrogen by 0.098 Å [Cu(1)] and 0.030 Å [Cu(2)] for **1**, 0.112 Å [Cu(1)] and 0.071 Å [Cu(2)] for **2**, 0.041 Å [Cu(1)] and 0.046 Å [Cu(2)] for **3**·2MeOH and 0.029 Å [Cu(1)] and 0.052 Å [Cu(2)] for **4**·2MeOH, respectively. There is a significant difference in the axial and equatorial Cu–N bond lengths. In each copper coordination site the equatorial Cu–N bond lengths are considerably longer than the corresponding axial Cu–N bond lengths. The Cu(1)···Cu(2) distances for the present complexes [3.225(3)–3.356(3) Å] are considerably longer than those found in analogous dimeric copper complexes bridged by two carboxylate groups where the Cu···Cu distances are in the 3.05–3.10 Å range.[15]

In **1**, **2**, **3**·2MeOH and **4**·2MeOH, the non-bonding ring–ring interactions are dominated by a stacking between the phen ligands. The shortest atom to atom distances within the stacking phen rings in each complex are in the 3.35–3.47 Å range. The dihedral angle between the two phen rings amounts to 9.0,

Table 2 Selected bond distances (Å) and angles (°) for **1**, **2**, **3**·2MeOH and **4**·2MeOH

	1	**2**	**3**·2MeOH	**4**·2MeOH
Cu(1)–O(1)	2.204(6)	2.247(10)	2.188(6)	2.191(11)
Cu(1)–N(1)	1.956(5)	1.967(9)	1.954(6)	1.921(12)
Cu(1)–N(3)	2.050(5)	2.035(9)	2.021(6)	2.006(13)
Cu(1)–N(5)	2.026(6)	2.044(9)	2.033(6)	2.026(12)
Cu(1)–N(6)	2.141(6)	2.083(8)	2.111(6)	2.101(12)
Cu(2)–O(4)	2.209(5)	2.215(8)	2.193(6)	2.192(13)
Cu(2)–N(2)	2.001(5)	2.015(9)	2.013(6)	2.025(12)
Cu(2)–N(4)	1.962(6)	1.946(9)	1.957(6)	1.948(12)
Cu(2)–N(7)	2.075(6)	2.104(8)	2.103(6)	2.106(13)
Cu(2)–N(8)	2.047(6)	2.047(8)	2.017(6)	2.025(13)
N(1)–N(2)	1.360(7)	1.366(11)	1.349(7)	1.371(15)
N(3)–N(4)	1.329(7)	1.356(11)	1.358(7)	1.368(15)
Cu(1)···Cu(2)	3.335(3)	3.356(3)	3.266(2)	3.225(3)
O(1)–Cu(1)–N(1)	92.3(2)	96.2(4)	93.3(2)	92.2(5)
O(1)–Cu(1)–N(3)	109.3(2)	95.3(4)	130.7(2)	129.9(5)
O(1)–Cu(1)–N(5)	90.3(2)	88.3(4)	90.2(2)	91.5(5)
O(1)–Cu(1)–N(6)	129.5(2)	126.6(4)	92.7(2)	93.2(5)
N(1)–Cu(1)–N(3)	90.3(2)	90.4(4)	89.8(2)	89.6(5)
N(1)–Cu(1)–N(5)	174.9(2)	172.4(4)	170.8(2)	170.7(5)
N(1)–Cu(1)–N(6)	94.8(2)	93.0(3)	90.8(2)	91.1(5)
N(3)–Cu(1)–N(5)	93.0(2)	95.4(4)	94.4(2)	94.5(5)
N(3)–Cu(1)–N(6)	120.5(2)	137.2(3)	136.5(2)	136.9(5)
N(5)–Cu(1)–N(6)	80.1(2)	79.4(4)	80.5(2)	80.2(5)
O(4)–Cu(2)–N(2)	103.3(2)	131.7(3)	130.0(2)	129.6(5)
O(4)–Cu(2)–N(4)	91.5(2)	92.7(3)	93.3(2)	92.8(5)
O(4)–Cu(2)–N(7)	112.7(2)	98.6(3)	91.1(2)	91.1(5)
O(4)–Cu(2)–N(8)	89.7(2)	89.6(3)	89.2(2)	89.8(5)
N(2)–Cu(2)–N(4)	90.7(2)	90.7(3)	90.3(2)	91.1(5)
N(2)–Cu(2)–N(7)	143.9(2)	129.4(3)	138.8(2)	139.1(5)
N(2)–Cu(2)–N(8)	97.5(2)	93.5(3)	94.9(2)	94.7(5)
N(4)–Cu(2)–N(7)	90.5(2)	92.8(3)	90.8(2)	90.6(5)
N(4)–Cu(2)–N(8)	171.1(2)	171.9(3)	170.8(2)	170.0(5)
N(7)–Cu(2)–N(8)	80.9(2)	79.3(3)	80.4(3)	79.6(5)
Cu(1)–N(1)–N(2)	122.3(4)	120.7(6)	118.9(4)	120.3(9)
Cu(1)–N(1)–C(1)	129.9(5)	131.8(8)	132.7(5)	134.2(11)
N(2)–N(1)–C(1)	107.6(5)	107.4(9)	108.2(5)	105.3(12)
Cu(2)–N(2)–N(1)	117.6(4)	119.2(6)	117.4(4)	115.7(9)
Cu(2)–N(2)–C(3)	133.5(5)	135.5(8)	135.0(5)	133.4(12)
N(1)–N(2)–C(3)	108.2(5)	105.4(9)	107.6(6)	110.9(13)
Cu(1)–N(3)–N(4)	119.2(4)	118.7(6)	115.7(4)	116.4(9)
Cu(1)–N(3)–C(4)	132.8(5)	131.9(8)	135.4(5)	135.2(11)
N(4)–N(3)–C(4)	107.9(5)	109.4(9)	108.7(6)	108.0(12)
Cu(2)–N(4)–N(3)	120.6(4)	121.6(7)	120.3(4)	119.7(9)
Cu(2)–N(4)–C(6)	129.2(5)	130.3(8)	131.0(5)	131.8(11)
N(3)–N(4)–C(6)	109.5(6)	107.9(9)	108.3(6)	108.4(12)

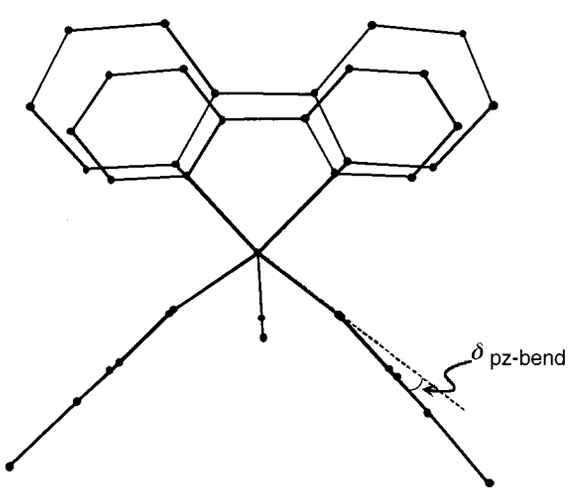

Fig. 2 Projection view through the Cu···Cu* direction of **5**.

6.8, 3.5 and 2.5° for **1**, **2**, **3**·2MeOH and **4**·2MeOH, respectively. On the other hand, **5** and **6** have no stacking interaction between the phen ligands because of the large dihedral angles of 67.3° for **5** and 56.3° for **6**. The projection of the structure for **5** along the Cu···Cu direction is shown in Fig. 2 by a wire-model. The average bending angles ($\delta_{pz\text{-}bend}$) of the pyrazolate least-squares plane to the Cu–N(pz)–N(pz)–Cu plane are in the 2.4–9.6° range.

Table 3 Selected bond distances (Å) and angles (°) for **5** and **6**

	5	**6**
Cu(1)–N(1)	1.976(3)	1.960(9)
Cu(1)–N(2)	1.964(3)	1.978(9)
Cu(1)–N(3)	2.038(4)	2.052(10)
Cu(1)–N(4)	2.022(3)	2.069(12)
Cu(1)–O(1)	2.223(3)	2.186(9)
N(1)–N(1*)	1.358(6)	1.334(17)
N(2)–N(2*)	1.356(7)	1.332(18)
Cu(1)···Cu(1*)	3.3024(10)	3.241(3)
N(1)–Cu(1)–N(2)	89.10(14)	90.7(4)
N(1)–Cu(1)–N(3)	164.31(14)	168.3(4)
N(1)–Cu(1)–N(4)	95.39(14)	92.1(5)
N(2)–Cu(1)–N(3)	93.39(14)	94.4(4)
N(2)–Cu(1)–N(4)	170.13(14)	159.8(4)
N(3)–Cu(1)–N(4)	79.95(14)	79.6(5)
O(1)–Cu(1)–N(1)	99.64(12)	94.6(3)
O(1)–Cu(1)–N(2)	95.49(13)	101.9(4)
O(1)–Cu(1)–N(3)	95.54(13)	94.6(4)
O(1)–Cu(1)–N(4)	92.41(13)	97.8(4)
Cu(1)–N(1)–N(1*)	119.47(9)	119.1(3)
Cu(1)–N(1)–C(1)	131.9(3)	132.6(9)
Cu(1)–N(2)–N(2*)	119.71(10)	118.8(3)
Cu(1)–N(2)–C(4)	131.5(3)	131.9(8)
C(1)–N(1)–N(1*)	107.7(2)	108.2(7)
C(4)–N(2)–N(2*)	107.9(2)	108.9(7)

* Symmetry operator: x, $1/2 - y$, z.

Table 4 Electronic spectral data for complexes **1**–**6**

Complex	$\tilde{\nu}_{max}/10^3$ cm^{-1}	$\tilde{\nu}_{sh}/10^3$ cm^{-1}	$\Delta\tilde{\nu}/10^3$ cm^{-1}
1	12.19	9.71	2.48
2	12.82	10.75	2.07
3	14.25	11.00	3.25
4	14.20	10.94	3.34
5	17.35	13.02	4.33
6	16.55	12.50	4.05

Electronic spectra

The reflectance spectral data for **1**–**6** are given in Table 4. The spectra of all the complexes show two absorptions in the visible region: a higher-energy absorption ($\tilde{\nu}_{max}$) at 12.19–17.35 × 10^3 cm^{-1} and a lower-energy shoulder ($\tilde{\nu}_{sh}$) at 9.71–13.02 × 10^3 cm^{-1}. It is known that the intensity of the shoulder on the lower-energy side increases and the separation of the two peaks, $\Delta\nu$, decreases when the distortion of the copper geometry from *SPY* towards *TBPY* increases.[16] Complex **2** (*TBPY* geometry, $\tau = 0.63$) has the smallest $\Delta\nu$ value of 2.07 × 10^3 cm^{-1}, and the intensities of the two absorptions become approximately the same (twin-peaked spectrum), whereas **5** (*SPY* geometry, $\tau = 0.10$) has the largest $\Delta\nu$ value of 4.33 × 10^3 cm^{-1}. As can be seen in Table 4, the $\Delta\nu$ value observed for the present complexes decreases in the following order: **5** > **6** > **4** > **3** > **1** > **2**. This order is just the same as that of the increase in the τ values for these complexes.

Magnetic properties

The magnetic properties of the present complexes are clearly of interest owing to the status of such complexes as novel examples of bis(μ-pyrazolato) bridged dimers with *TBPY* or *SPY* copper configurations. The observed magnetic susceptibility data were fitted to the modified Bleaney–Bowers eqn. (2) by allowing for the presence of monomer impurity,[17] where p is the

Table 5 Magnetic data for complexes **1**–**6**

Complex	g	$-2J$/cm^{-1}	p (%)	μ_{eff}/μ_B (T/K)	$\sigma_{dis} \times 10^2$
1	2.14	143	0	1.67 (300.0)	0.37
2	2.18	166	0	1.64 (289.0)	0.46
3	2.24	238	0	1.55 (292.5)	0.92
4	2.21	227	1.6	1.56 (294.8)	0.49
5	2.23	244	0.7	1.53 (290.0)	0.70
6	2.25	268	0.9	1.50 (286.4)	0.47

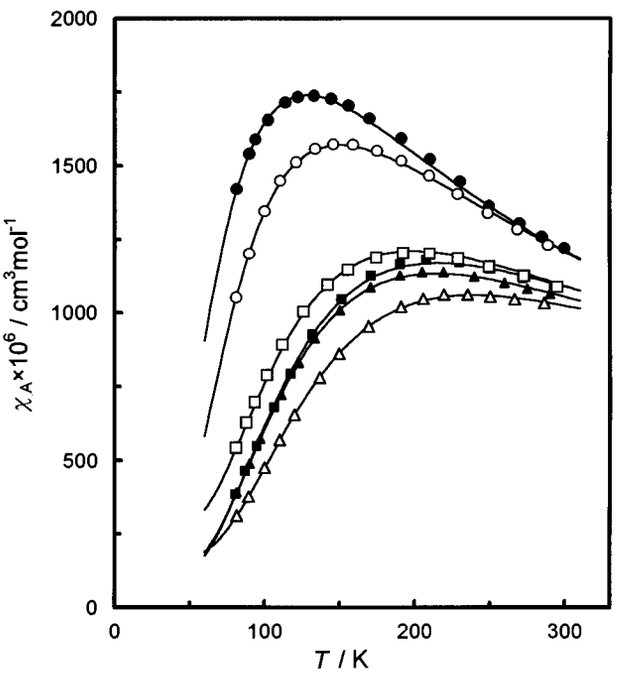

Fig. 3 Temperature dependence of magnetic susceptibilities for **1** (●), **2** (○), **3** (■), **4** (□), **5** (▲) and **6** (△). The solid curves were obtained as described in the text.

$$\chi_A = \left(\frac{Ng^2\beta^2}{kT}\right)\left[3 + \exp\left(\frac{-2J}{kT}\right)\right]^{-1}(1-p) + \left(\frac{Ng_i^2\beta^2}{4kT}\right)p + Na \quad (2)$$

mole fraction of the non-coupled copper(II) impurity and g_i is the average g factor for the impurity. The values of g_i of 2.2 and Na of 60×10^{-6} cm^3 mol^{-1} were used throughout the present study. The best-fit parameters of $-2J$ and g were obtained by a nonlinear least-squares fitting procedure. The quantity of fit was estimated by means of a discrepancy index [eqn. (3)].

$$\sigma_{dis} = \sqrt{\frac{\Sigma(\chi_{obsd} - \chi_{calcd})^2}{\Sigma\chi_{obsd}{}^2}} \quad (3)$$

The magnetic data are given in Table 5 and are represented graphically in Fig. 3. The magnetic data for **1**–**6** are well represented by eqn. (2), indicating that an antiferromagnetic interaction is operative between the copper(II) ions in these complexes.

The complexes described here can be classified into two groups based on the magnetic data and the τ values. Group A: in **1**, **2**, **3** and **4**, the τ values are 0.54–0.63, and the $-2J$ values fall in the 143–238 cm^{-1} range. Group B: in **5** and **6**, the τ values are 0.10 and 0.14, respectively, and the $-2J$ values are evaluated to 244 cm^{-1} for **5** and 268 cm^{-1} for **6** which are definitely larger than those of group A.

The appropriate comparisons of the present complexes with other binuclear complexes containing pyrazolate moieties are informative. The $[Cu(L^1)(L^2H)_2]_2$ complex (where L^1 = 4-bromo-3-carboxylato-5-methylpyrazolate and L^2 = 4-bromo-3,5-dimethylpyrazolate), has pyrazolate-bridges with a CO_2 chelating arm, and has distorted *TBPY* copper centers.[5d] The magnitude of the exchange coupling in this complex ($-2J$ = 150.8 cm^{-1}) is equivalent to that for **1** and **2** of group A. The $[Cu_2(L)(pz)_2]$-$[ClO_4]_2$ (where L = 20-membered N_4 macrocycle; $-2J$ = 270 cm^{-1})[6] and $[\{H_2B(pz)_2\}Cu(pz)_2(X^1)Cu\{H_2B(pz)_2\}]X^2$ (where X^1, X^2 = Cl, PPh_4 or Br, $AsPh_4$; $-2J$ = 241–244 cm^{-1})[3f] complexes also have a pyrazolate-bridged dicopper core in which the primary pathway for the magnetic interaction must be through pyrazolate-bridges. The former complex has a binucleating macrocycle, and the coordination environment of each copper ion was described as a square-planar geometry though the percholate anion was weakly attracted to the copper atom in an axial position. For the latter complex, a distorted *SPY* having one exogenous bridging halide ion in the axial position was assigned. The $-2J$ values for these complexes are identical with those for the complexes of group B. The $[Cu_2L_2][BPh_4]_2$ complexes (where L = pyrazole ligands with nitrogen-containing chelating arms) have been reported as the "first example" of pyrazolate-bridged binuclear copper(II) complexes.[5a] The complexes have a square-planar geometry around each copper(II) ion, and have larger $-2J$ values (362–428 cm^{-1}) than those for the complexes of group B. Some of this difference or similarity in the strength of the antiferromagnetic interaction may be accounted for by the coordination geometry. In the complexes classified into group A, the magnetic orbital is the d_{z^2} orbital and the pyrazolate groups such that one nitrogen occupies an axial site on one copper ion while the other nitrogen occupies an equatorial site on the other copper ion in the molecule. The overlap of the magnetic d_{z^2} orbitals with ligand orbitals in the xy plane is expected to be weaker and less effective than that in the complexes classified into group B with the $d_{x^2-y^2}$ orbital as the magnetic orbital and the bridging ligands bonded in the xy plane. Therefore, the strength of the antiferromagnetic interaction in pyrazolate-bridged binuclear copper(II) complexes with five-coordination decreases as the distortion of copper(II) geometry increases from *SPY* toward *TBPY*. There exists, however, less correlation between the τ value and the strength of the antiferromagnetic interaction in **1**–**6**; the $-2J$ value of **2** is larger than that of **1**, whereas the τ value of **2** is smaller than that of **1**. Moreover, complexes **3** and **4** have almost the same τ values as each other, whereas the $-2J$ value of **3** is larger by 11 cm^{-1} than that of **4**. In order to explain these inconsistencies, the dihedral angle ($\delta_{pz\text{-}bend}$) of the least-square plane of pz relative to the Cu–N(pz)–N(pz)–Cu plane is proposed as a new structural factor affecting the magnetic interactions (Table 6, Chart 1). The $-2J$ value is expected to decrease as the $\delta_{pz\text{-}bend}$ bending angle becomes larger, because the magnetic d_{z^2} or $d_{x^2-y^2}$ orbital gives a much smaller overlap with the pz ligand orbital when $\delta_{pz\text{-}bend}$ is large. In comparison with the $\delta_{pz\text{-}bend}$ values for each pair of the complexes having almost identical τ values, the $-2J$ values become smaller as the $\delta_{pz\text{-}bend}$ values become greater; the $\delta_{pz\text{-}bend}$ values of **1** > **2** (τ = 0.61, 0.63), **4** > **3** (τ = 0.54, 0.55) and **5** > **6** (τ = 0.10, 0.14). Accordingly, τ is a leading factor in determining the $-2J$ value, and the bending angle ($\delta_{pz\text{-}bend}$) plays an important supporting role. This effect of bending angle in bridging ligands on the antiferromagnetic interaction has also been observed in binuclear copper(II) benzoate complexes.[18] Ajò *et al.*[3f] have performed extended-Hückel calculations on the model complex $[Cu_2(pz)_2Cl_4]^{2-}$, to estimate the effects of deviations from coplanarity on the antiferromagnetic interaction in bis(pyrazolato)-bridged copper(II) dimers. They suggested that a strong antiferromagnetic interaction through the pyrazolate bridge is observed when both the dihedral angle δ between the two $CuCl_2$ planes and the dihedral angle δ' ($=\delta_{pz\text{–}pz}$) between the planes of the pyrazole molecules are equal to 180°. Furthermore, they pointed out that for δ = 90 and δ' = 90 the antiferromagnetic interaction is estimated to be even larger than that calculated in the planar situation. In the present complexes, however, $\delta_{CuNN'}$ (the dihedral angle between the $CuN_{pz}N_{pz'}$ planes) which

Table 6 A comparison of $-2J$ with structural parameters for complexes **1**–**6**

Complex	$-2J$/cm^{-1}	$\tau_{av\ (\tau Cu1,\ \tau Cu2)}$	$\delta_{pz\text{-}bend}$ [a]/°	$\delta_{pz\text{–}pz}$ [a]/°	$\delta_{CuNN'}$ [a]/°
1	143	0.61 (0.76, 0.45)	6.6 (6.1, 7.1)	110.3	90.5
2	166	0.63 (0.59, 0.67)	2.4 (2.0, 2.9)	106.9	90.8
3	238	0.55 (0.57, 0.53)	3.9 (2.8, 5.0)	112.2	83.7
4	227	0.54 (0.56, 0.52)	4.5 (3.4, 5.6)	113.1	83.7
5	244	0.10	9.6 (9.7, 9.5)	88.3	87.7
6	268	0.14	4.1 (1.4, 6.8)	100.7	87.1

[a] See Chart 1.

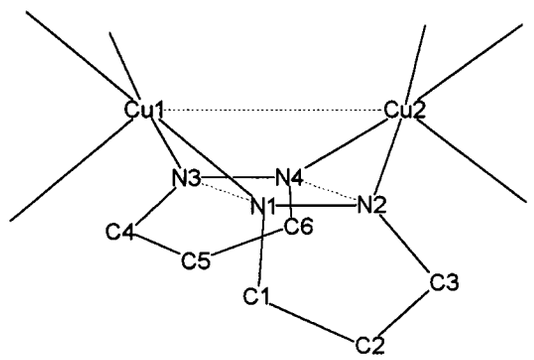

Dihedral angle	[plane]	—	[plane]
$\delta_{pz-bend}$	[N1-C1-C2-C3-N2]	—	[Cu1-N1-N2-Cu2]
	[N3-C4-C5-C6-N4]	—	[Cu1-N3-N4-Cu2]
δ_{pz-pz}	[N1-C1-C2-C3-N2]	—	[N3-C5-C6-C7-N4]
$\delta_{CuNN'}$	[Cu1-N1-N3]	—	[Cu2-N2-N4]

Chart 1

corresponds to δ in the model complex and δ' fall into the 83.7–90.8 and 88.3–113.1° ranges, respectively (Table 6), and no calculation was reported for such ranges. Thus, we have carried out the extended-Hückel calculations on the model complex $[Cu_2(pz)_2Cl_4]^{2-}$ having such δ and δ' ranges by a method similar to that described by Ajò. The energy separation ($\Delta\varepsilon$) between symmetric HOMO (φ_s) and asymmetric HOMO (φ_a) for $[Cu_2(pz)_2Cl_4]^{2-}$ with such δ and δ' ranges falls into the very narrow 0.15–0.16 eV range. These calculations clearly show that the estimated $\Delta\varepsilon$ for the model complex is not the dominant factor in determining the order of the $-2J$ values for the present complexes. Consequently, the antiferromagnetic interaction in the present complexes is closely related to the coordination geometry around the copper ion, and an additional effect for the magnetic interaction must be the bending angle of the bridging pyrazolate.

Acknowledgements

This work was supported by Grants-in-Aid for Science Research (B) (No. 10440196) and Grants-in-Aid for Scientific Research on Priority Areas (No. 10149240 "Metal-assembled Complexes") from the Ministry of Education, Science, Sports and Culture of Japan.

References

1 D. J. Hodgson, *Prog. Inorg. Chem.*, 1975, **19**, 173; V. H. Crawford, H. W. Richardson, J. R. Wasson, D. J. Hodgson and W. E. Hatfield, *Inorg. Chem.*, 1976, **15**, 2107; P. J. Hay, J. C. Thibeault and R. Hoffmann, *J. Am. Chem. Soc.*, 1975, **97**, 4884.
2 S. Trofimenko, *Chem. Rev.*, 1972, **72**, 497; *Prog. Inorg. Chem.*, 1986, **34**, 115; M. Inoue and M. Kubo, *Coord. Chem. Rev.*, 1976, **21**, 1.
3 (*a*) W. Mazurek, B. J. Kennedy, K. S. Murray, M. J. O'Connor, J. R. Rodgers, M. R. Snow, A. G. Wedd and P. R. Zwack, *Inorg. Chem.*, 1985, **24**, 3258; W. Mazurek, A. M. Bond, M. J. O'Connor and A. G. Wedd, *Inorg. Chem.*, 1986, **25**, 906; Y. Nishida and S. Kida, *Inorg. Chem.*, 1988, **27**, 447; T. N. Doman, D. E. Williams, J. F. Banks, R. M. Buchanan, H.-R. Chang, R. J. Webb and D. N. Hendrickson, *Inorg. Chem.*, 1990, **29**, 1058; (*b*) R. Robson, *Aust. J. Chem.*, 1970, **23**, 2217; W. D. McFayden, R. Robson and H. Schaap, *Inorg. Chem.*, 1972, **11**, 1777; H. P. Berends and D. W. Stephan, *Inorg. Chem.*, 1987, **26**, 749; (*c*) P. Iliopoulos, G. D. Fallon and K. S. Murray, *J. Chem. Soc., Dalton Trans.*, 1988, 1823; (*d*) P. Iliopoulos, K. S. Murray, R. Robson, J. Wilson and G. A. Williams, *J. Chem. Soc., Dalton Trans.*, 1987, 1585; (*e*) T. Kamiusuki, H. Ōkawa, E. Kitaura, M. Koikawa, N. Matsumoto, H. Oshio and S. Kida, *J. Chem. Soc., Dalton Trans.*, 1989, 2077; (*f*) D. Ajò, A. Bencini and F. Mani, *Inorg. Chem.*, 1988, **27**, 2437.
4 M. K. Ehlert, S. J. Rettig, A. Storr, R. C. Thompson and J. Trotter, *Can. J. Chem.*, (*a*) 1989, **67**, 1970; (*b*) 1991, **69**, 432; (*c*) M. K. Ehlert, A. Storr and R. C. Thompson, *Can. J. Chem.*, 1992, **70**, 1121.
5 (*a*) T. Kamiusuki, H. Ōkawa, N. Matsumoto and S. Kida, *J. Chem. Soc., Dalton Trans.*, 1990, 195; (*b*) T. Kamiusuki, H. Ōkawa, H. Inoue, N. Matsumoto, M. Kodera and S. Kida, *J. Coord. Chem.*, 1991, **23**, 201; (*c*) J. C. Bayon, P. Esteban, G. Net, P. G. Rasmussen, K. N. Baker, C. W. Hahn and M. M. Gumz, *Inorg. Chem.*, 1991, **30**, 2572; (*d*) M. K. Ehlert, S. J. Retting, A. Storr, R. C. Thompson and J. Trotter, *Can. J. Chem.*, 1992, **70**, 2161; (*e*) J. Pons, X. López, J. Casabó, F. Teixidor, A. Caubet, J. Rius and C. Miravitlles, *Inorg. Chim. Acta*, 1992, **195**, 61; (*f*) B. Mernari, F. Abraham, M. Lagrenee, M. Drillon and P. Legoll, *J. Chem. Soc., Dalton Trans.*, 1993, 1707; (*g*) F. Degang, W. Guoxiong, Z. Zongyuan and Z. Xiangge, *Transition Met. Chem.*, 1994, **19**, 592; (*h*) M. Kumar, V. J. Arán, P. Navarro, A. Ramos-Gallardo and A. Vegas, *Tetrahedron Lett.*, 1994, **35**, 5723; (*i*) V. P. Hanot, T. D. Robert, J. Kolnaar, J. G. Haasnoot, J. Reedijk, H. Kooijman and A. L. Spek, *J. Chem. Soc., Dalton Trans.*, 1996, 4275; (*j*) F. Meyer, A. Jacobi and L. Zsolnai, *Chem. Ber./Recl.*, 1997, **130**, 1441.
6 M. G. B. Drew, P. C. Yates, F S. Esho, J. Trocha-Grimshaw, A. Lavery, K. P. Mckillop, S. M. Nelson and J. Nelson, *J. Chem. Soc., Dalton Trans.*, 1988, 2995.
7 P. W. Selwood, *Magnetochemistry*, Interscience, New York, 1956, pp. 78 and 91.
8 C. J. Gilmore, MITHRIL, *J. Appl. Crystallogr.*, 1984, **17**, 42; P. T. Beurskens, DIRDIF, Technical Report 1984/1, Crystallography Laboratory, Toernooiveld, Nijmegen, 1984.
9 Function minimized: $\sum w(|F_o| - |F_c|)^2$, where $w = 4F_o^2/\sigma^2(F_o^2)$. Standard deviation of an observation of unit weight: $[\sum w(|F_o| - |F_c|)^2/(N_o - N_v)]^{\frac{1}{2}}$, where N_o = number of observations, N_v = number of variables.
10 D. T. Cromer and J. T. Waber, *International Tables for X-Ray Crystallography*, Kynoch Press, Birmingham, 1974, vol. 4, Table 2.2A.
11 J. A. Ibers and W. C. Hamilton, *Acta Crystallogr.*, 1964, **17**, 781.
12 D. T. Cromer, *International Tables for X-Ray Crystallography*, Kynoch Press, Birmingham, 1974, vol. 4, Table 2.3.1.
13 TEXSAN-TEXRAY Structure Analysis Package, Molecular Structure Corporation, Houston, TX, 1985.
14 A. W. Addison, T. N. Rao, J. Reedijk, J. van Rijn and G. C. Verschcoor, *J. Chem. Soc., Dalton Trans.*, 1984, 1349.
15 T. Tokii, N. Watanabe, M. Nakashima, Y. Muto, M. Morooka, S. Ohba and Y. Saito, *Chem. Lett.*, 1989, 1671; *Bull. Chem. Soc. Jpn.*, 1990, **63**, 364.
16 A. A. G. Tomlinson, B. J. Hathaway, D. E. Billing and P. Nicholls, *J. Chem. Soc. A*, 1969, 65.
17 B. Bleaney and K. D. Bowers, *Proc. R. Soc. London, Ser. A*, 1952, **214**, 451.
18 M. Yamanaka, H. Uekusa, S. Ohba, Y. Saito, S. Iwata, M. Kato, T. Tokii, Y. Muto and O. W. Steward, *Acta Crystallogr., Sect. B*, 1991, **47**, 344.

Paper 8/08074G